Correlations between the alpha particles and ejectiles in the reaction ^{93}Nb+ ^{14}N at $E_{lab}=208$ MeV

T. Fukuda,[a] M. Ishihara,[b] M. Tanaka,[c] I. Miura,[d] H. Ogata,[d] and H. Kamitsubo[b]
[a]*Department of Physics, Osaka University, Toyonaka, Osaka 560, Japan*
[b]*Institute of Physical and Chemical Research, Wako-shi, Saitama 351, Japan*
[c]*Kobe Tokiwa Junior College, Nagata, Kobe 653, Japan*
[d]*Research Center for Nuclear Physics, Osaka University, Suita, Osaka 565, Japan*
(Received 11 May 1981)

The correlations between alpha particles and various ejectiles were investigated in the reaction ^{93}Nb+ ^{14}N at $E_{lab}=208$ MeV. The ejectiles were measured at a fixed angle $\theta_1=+22°$, which was slightly more backward than the grazing angle, and the alpha particles were measured at various angles θ_2 in and out of the reaction plane. The experimental results were analyzed in terms of various aspects of the correlations such as the energy and angular correlations, the projected energy spectra, and differential multiplicities. An analysis based on the three body kinematics was also made to study the features associated with the sequential ejectile breakup process. It was found that two processes contribute to the coincident alpha particles. The first process was ascribed to the sequential breakup of the excited ejectiles and was found to be dominant in the angular region of θ_2 close to the ejectile detector. The coincidence cross section of the sequential breakup component can be approximately factorized as a product of the singles cross section of excited ejectiles before breakup and the excitation spectrum of the ejectiles. The other process, ascribed to a nonsequential mechanism, was dominant for the alpha particles detected on the opposite side of the ejectile detector with respect to the beam direction. This process is characterized by the following properties: (i) The energy spectra of the coincident alpha particles have shapes which are almost identical to those of the singles spectra taken at the same angles. (ii) The same is true to a lesser extent for the ejectile spectra except for the higher-energy region. (iii) In this angular region of θ_2 the differential coincidence cross section can be approximately expressed in the factorization form, $d^4\sigma/d\Omega_1 d\Omega_2 dE_1 dE_2 = K\cdot(d^2\sigma/d\Omega_1 dE_1)(d^2\sigma/d\Omega_2 dE_2)$. The relative contribution of the two processes was found to be roughly comparable.

[NUCLEAR REACTIONS ^{93}Nb(^{14}N,HIα), $E=208$ MeV; measured two-dimensional HI-α coincident energy and angular correlations; deduced reaction mechanisms.]

I. INTRODUCTION

Extensive studies[1-23] of particle-particle correlations have been made recently for heavy-ion damped reactions. It has been shown widely that large fractions of projectilelike fragments (ejectiles) are accompanied by emissions of light particles such as alpha particles and nucleons. Such coincident particles are often characterized by large kinetic energies and strongly focused angular correlations relative to the ejectiles. These features are particularly dominant for reactions induced by relatively light projectiles[1-17] ($A \lesssim 20$), whereas in heavier systems[18-23] ($A \gtrsim 40$) it is less significant and coincident light particles are usually attributed simply to equilibrium emissions from reaction residues. A variety of theoretical studies[24-26] have sought emission mechanisms that could explain these features of the coincident particles. These theories have been sometimes successful in accounting for observed correlations, but no overall understanding of the phenomena has been so far achieved. It appears that several different mechanisms may coexist in a reaction and their relative importance may differ between different reaction systems. It would thus be important to study a

 ©1982 The American Physical Society

variety of reactions with different energies and projectiles so as to gain further insight into the three body process. In this paper we present the results on the correlations between alpha particles and ejectiles in the reaction ^{93}Nb+ ^{14}N at $E_{lab}=208$ MeV.

It is rather surprising that a large number of different mechanisms have been conjectured to account for the origin of the coincident light particles, which often exhibit seemingly common features. For one thing this may be related to the versatile nature of the damped reactions, in which the light particles can conceivably be emitted at any stage of the multistep scattering process and from a variety of sites of colliding nuclei. On the other hand, it also appears possible that insufficient experimental data and lack of analysis of the inherently complex three body final channels have allowed ambiguous interpretations and even incorrect conclusions. Thus in the present work a strong effort was made to obtain data with sufficient statistics and then to carry out the three body kinematic analysis as thoroughly as possible.

A list of plausible emission mechanisms so far proposed for the coincident light particles includes: (i) sequential breakup of the excited ejectiles (Refs. 5, 10, 12, 13, 15, 16), (ii) preequilibrium emission from a locally heated zone (hot spot) in the targetlike fragments,[3,4,25,26] (iii) prompt emission caused by radial friction (piston model),[24] (iv) emission in neck rupture of the dinuclear systems, which is analogous to the ternary fission process accompanying a long-range alpha particle, and (v) fast particle emission to be associated with the projectile fragmentation process.[8,15,17] Mechanism (iii) has been also discussed in terms of "Fermi jet"[27,28] or the "promptly emitted particle" process.[29,30] These mechanisms may be classified according to the stage of the damped reactions when the light particles are emitted. Mechanisms (iii) and (v) are supposed to occur prior to or in a very early stage of the reactions, while (i) and (ii) occur after the damped reactions are completed, (iv) being at the last stage of the damped reactions. The emission mechanisms may also be classified according to the species emitting the particles. Mechanisms (i) and (v) are relevant to the projectile or projectilelike fragments, (ii) mainly to the targetlike fragments, and the rest to the neck region of the dinuclear composite systems.

It has been shown recently that preequilibrium emission of light particles is an important aspect of inclusive spectra of heavy-ion reactions.[31–46] These light particles have characteristics similar to the coincident light particles, favoring high energies and forward peaked angular distributions. Naturally, the link between the singles and coincidence phenomena has been sought; the approaches in terms of mechanisms (ii),[25,26,47,48] (iii),[24,27–30] and (v) emphasize this aspect.

Among the various proposed mechanisms, only two have achieved accumulating evidence to support their significance, whereas most of the others still lack solid experimental verification. One important mechanism is the sequential breakup of the ejectiles. The first evidence for this mechanism was reported for the reaction ^{93}Nb+ ^{14}N at $E_{lab}=90$ and 110 MeV.[5] It was found that most of the coincident alpha particles can be attributed to the sequential process on the basis of three body kinematic analysis. Similar conclusions were obtained about the coincident alpha particles from ^{16}O induced reactions such as ^{197}Au+ ^{16}O at 310 MeV,[13] ^{93}Nb+ ^{16}O at 204 MeV,[10] and ^{27}Al+ ^{16}O at 88 MeV.[16]

The other important mechanism appears to be the "fragmentationlike" mechanism of category (v) which was discussed by Bhowmik *et al.*[8,17] for the reaction ^{58}Ni+ ^{14}N at 148 MeV. They pointed out that the cross section for coincidences between alpha particles and ejectiles may be factorized as a product of singles cross sections for the two coincident particles as given by

$$d^4\sigma/d\Omega_1 d\Omega_2 dE_1 dE_2 = K\cdot(d^2\sigma/d\Omega_1 dE_1)_{\text{singles}} \times (d^2\sigma/d\Omega_2 dE_2)_{\text{singles}}\ , \quad (1)$$

where K is a constant. Based on this observation they inferred that the reaction proceeds in two stages: First the alpha particle is emitted in a fragmentationlike process, and then the rest of the projectile undergoes the reaction with the target nucleus.

Towards the end of this paper we shall show that the above two mechanisms coexist in the presently studied reaction. However, the process, which we symbolically refer to as the fragmentationlike mechanism, showed only partial resemblance to the process characterized by the factorization formula of Eq. (1).

In Sec. II the experimental procedures are described. The experimental results are presented in Sec. III. Various aspects of the data are found to support the coexistence of two reaction mechanisms. In Sec. IV we perform three body kinematic analysis, which is used to study the features of the

sequential breakup mechanism. In Sec. V, an attempt is made to isolate the contributions from the two mechanisms in order to see their relative importance. A similar attempt was made recently[15] for the ^{159}Tb+ ^{14}N reaction, but the conclusions are somewhat different. The summary and discussion are given in Sec. VI.

II. EXPERIMENTAL PROCEDURES

The experiment was performed at the 230-cm AVF cyclotron of the Research Center for Nuclear Physics at Osaka University. A ^{93}Nb metallic foil of 4.8-mg/cm^2 thickness was bombarded by a 208-MeV ^{14}N beam. Projectilelike fragments were identified by a conventional 30-μm E and 5000-μm E Si telescope, which distinguished individual isotopes of elements from $Z=3$ to $Z=6$. This telescope subtended a solid angle of $\Omega=3.6$ msr and an angle of $\Delta\theta=\pm1.6°$ in the reaction plane. The telescope was placed at an angle of $\theta_1=+22°$, which was slightly more backward than the grazing angle ($\theta_{gr}\simeq11°$). This choice was made partly because the fully damped (deep inelastic) components were almost as significant as the quasielastic components at that angle. Four identical triplet telescopes, which consisted of 30-μm ΔE_1, 300-μm ΔE_2, and 5000 (or 3000)-μm E Si detectors, were used to detect coincident alpha particles with energies from 6 to 100 MeV. The angular correlations were measured by placing these detectors at angles θ_2 between $-50°$ and $+60°$ and at $-160°$ in the reaction plane, which was defined by the beam axis and the direction of the fixed telescope. Out of plane correlations were measured on meridians which cut the reaction plane at $\theta_2=+11°$ and $-15°$. These telescopes typically subtended solid angles of 2.0 and 6.4 msr and angles of $\pm1.2°$ and $\pm2.2°$ at the forward and backward angles θ_2, respectively. For the measurement at $\theta_2=+8°$ and $-8°$, an aluminum absorber of 0.5-mm thickness was placed in front of the telescope to eliminate the huge disturbance from elastically scattered particles, resulting in the cutoff of the alpha particles below 35 MeV. Distortion of the energy spectra due to the absorber was corrected by using the range-energy relation of Ref. 49.

A set of six signals consisting of $(\Delta E,E)$ of projectilelike fragments, $(\Delta E_1,\Delta E_2,E)$ of alpha particles, and the timing, time-to-amplitude converter (TAC) between two telescopes was stored event by event on magnetic tape and was analyzed off line. Random coincident events were subtracted.

The amounts of carbon and oxygen contaminants in the target were estimated to be less than 3 and 5 μg/cm^2 based on a measurement on the elastic scattering of 120-MeV alpha particles. The coincidence cross sections were measured for carbon and Mylar targets in order to evaluate the contributions from the carbon and oxygen contaminants. They were found to be less than 5% of the total coincident events for most of the different coincidence settings and no correction was made for simplicity.

The absolute magnitude of the cross section was determined within 10%; the error bars drawn in figures are due to statistical errors.

III. EXPERIMENTAL RESULTS

In this section we present experimental results. Various aspects of the correlations are discussed in separate subsections. Some other aspects are also described in Secs. IV B and IV C, where the data were analyzed in terms of three body kinematics. Throughout these aspects one persistent feature is apparent, i.e., the behavior of the correlations is distinctively different between two angular regions of the alpha particle detection, one (region I) being closer to the angle θ_1 of the ejectile, and the other (region II) further towards the opposite side of the beam axis. Though the boundary of the two regions is somewhat uncertain, it may be roughly set at $\theta_2=0°$, i.e., the beam direction. The particles involved in the three body final channels are labeled by numbers: 1, for the projectilelike fragments (detected ejectiles), 2, for the alpha particles, and 3, for the targetlike fragments (unobserved recoil nuclei). The singles cross section is distinguished by the subscript "singles." Otherwise σ refers to the coincidence cross section.

A. The velocity plot of the coincident alpha particles

The overall feature of the energy and angular correlations may be best seen in a plot of the Galilei invariant coincidence cross section on the velocity plane with coordinates of longitudinal ($v_{||}$) and transverse ($v_\perp$) components of the velocity $\vec{v}_2$ of the coincident alpha particles. A typical example of such a plot is shown in Fig. 1 for the ^{12}C channel. The plotted cross section $d^3\sigma/d\Omega_1 d\Omega_2 dv_2{}^3$ is integrated over the energy of

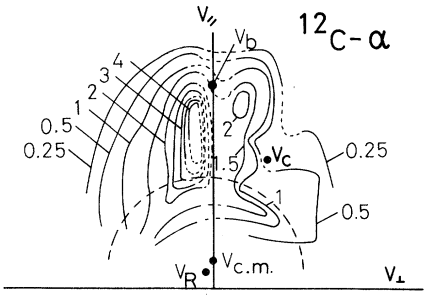

FIG. 1. The contour plot of the Galilei invariant coincidence cross section $d^3\sigma/d\Omega_1 d\Omega_2 dv_2{}^3$ on the velocity plane with coordinates of longitudinal ($v_{||}$) and transverse ($v_{\perp}$) components of the velocity $\vec{v}_2$ of alpha particles coincident with ^{12}C ions. The dotted lines indicate smooth continuations of the data points. Reference vectors are shown together to represent the velocities of the beam ($\vec{v}_b$), the coincident ^{12}C and the corresponding recoil nucleus with their mean kinetic energies ($\vec{v}_c$ and $\vec{v}_R$, respectively), and the center of mass of the total system ($\vec{v}_{c.m.}$). The contours are expressed in units of b/sr$^2c^3$, where c is the velocity of the light. The dashed line centered around the top of $\vec{v}_R$ represents the most probable velocity expected for the equilibrium evaporation from the targetlike fragment (see text).

the ejectile (^{12}C). Some reference vectors are shown together to represent the velocities of the beam ($\vec{v}_b$), the coincident ^{12}C and the corresponding recoil nucleus with their mean kinetic energies ($\vec{v}_c$ and $\vec{v}_R$, respectively), and the center of mass of the total system ($\vec{v}_{c.m.}$).

The following observations are made: (i) Most of the coincidence events are distributed in the region of velocity much larger than that expected for the equilibrium evaporation from the targetlike fragment. The typical velocity for the equilibrium evaporation is depicted in Fig. 1 by a dashed line centered around $\vec{v}_R$. The corresponding energy is given by the temperature of 3 MeV (deduced from the data at $\theta_2 = -160°$) plus Coulomb barrier energy between the alpha particle and targetlike fragment. The above feature imples that the equilibrium alpha emission from the heavy residue is not as important in the present reaction as in the reaction systems between heavier ions ($A \gtrsim 40$).[18] (ii) The favored direction of the coincidence cross section does not coincide with either the direction of the ^{12}C or of the recoil nucleus. In some of the earlier papers,[3,4] the enhanced yield of fast alpha particles in the direction of the recoil nucleus was reported and was interpreted as a strong indication of the hot spot formation in the recoil nucleus. This feature is absent in the present system. (iii) The pattern of the yield distribution is distinctively different between regions I and II. For instance, several local peaks are observed in region I, which do not have any correspondent peaks on the opposite side with respect to the beam direction. This observation clearly conflicts with the simple factorization formula of Eq. (1), which implies that the coincidence cross section should be symmetric with respect to the beam direction. However we will show later that the data of region II ($\theta_2 < 0°$) are generally consistent with the features of Eq. (1), and that the structured distribution of region I ($\theta_2 > 0°$) is indicative of the sequential breakup of the projectilelike fragment.

B. Angular distributions

The energy integrated in-plane angular distributions of the alpha particles in coincidence with different ejectiles are shown in Fig. 2. The distributions are all peaked around angles rather close to the beam direction. Strictly speaking, the distributions are not necessarily symmetric with respect to the beam direction and the peak angles vary for different ejectiles. Correspondingly, the ratios σ_I/σ_{II} of the coincidence cross section of region I to that of region II vary rather strongly with the coincident ejectiles; they increase from ~ 0.6 to ~ 2 as the ejectile varies from carbon to lithium. This variation may be related to the balance between the two competing mechanisms which are, respectively, dominant in regions I and II.

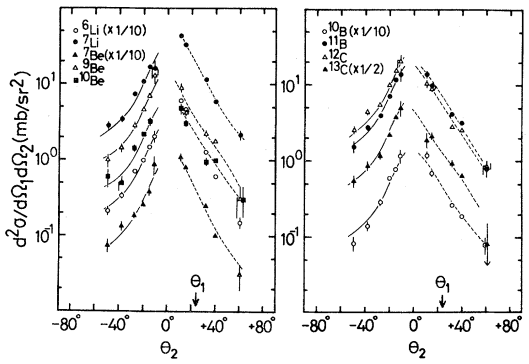

FIG. 2. The energy integrated in-plane angular distribution of the alpha particles coincident with various ejectiles as a function of lab angle θ_2. The ejectiles were detected at a fixed angle $\theta_1 = +22°$. The solid lines represent the angular dependence of the singles cross section of the alpha particles. The dashed lines are drawn to guide the eye.

In Sec. V C, we attempt to decompose the angular distributions into two components corresponding to two different reaction mechanisms. A similar analysis was made recently for the data of the ^{159}Tb+ ^{14}N reaction.[15] In that analysis they assumed a component due to the ejectile breakup contributed along with a fragmentationlike component, which followed the dependency expressed by Eq. (1). We note, however, that this assumption is not appropriate for the present reaction, since the observed ratio $\sigma_{\rm I}/\sigma_{\rm II}$ is often below unity, while $\sigma_{\rm I}/\sigma_{\rm II} \geq 1$ would result from this assumption.

The solid lines in Fig. 2 represent the angular dependence of the singles cross section of the alpha particles. They follow the coincidence data of region II rather well irrespective of the final channels, i.e., the factorization formula of Eq. (1) approximately holds at least for region II. A related discussion is made in Sec. III D.

C. Energy correlations

The energy correlations between the alpha particles and ejectiles may be seen in the plot of the coincidence yield for a given set of (θ_1,θ_2) over the plane of ejectile energy (E_1) vs alpha particle energy (E_2). Figure 3 shows such plots for data of the α+ ^{12}C channel taken at $\theta_1 = +22°$ and $\theta_2 = +15°$, $+32°$, and $-20°$. For the case of $\theta_2 = +15°$ and $+32°$ (region I), two local maxima are observed, whereas a smooth distribution is seen for $\theta_2 = -20°$ (region II). It is apparent that the two humped structure in region I is not expected from the simple factorization formula of Eq. (1). On the other hand, such structure was observed experimentally in an earlier study[5] of the ^{93}Nb(^{14}N,HIα) reaction at lower incident energies of 90 and 110 MeV, where the result was interpreted as due to the ejectile breakup process on the basis of the three body kinematic analysis. In the present paper we have also performed the three body kinematic analysis as described in detail in Sec. IV. Below we only quote some qualitative conclusions drawn on the significance of the two humped structure.

The dashed lines and solid lines shown in Fig. 3 represent, respectively, the loci of the relative kinetic energy E_{1-2} between the alpha particle and ^{12}C and of the relative kinetic energy E_{12-3} between the center of mass of the composite system (α+ ^{12}C= ^{16}O in this case) and its recoil nucleus, respectively. It can be seen that the cross section

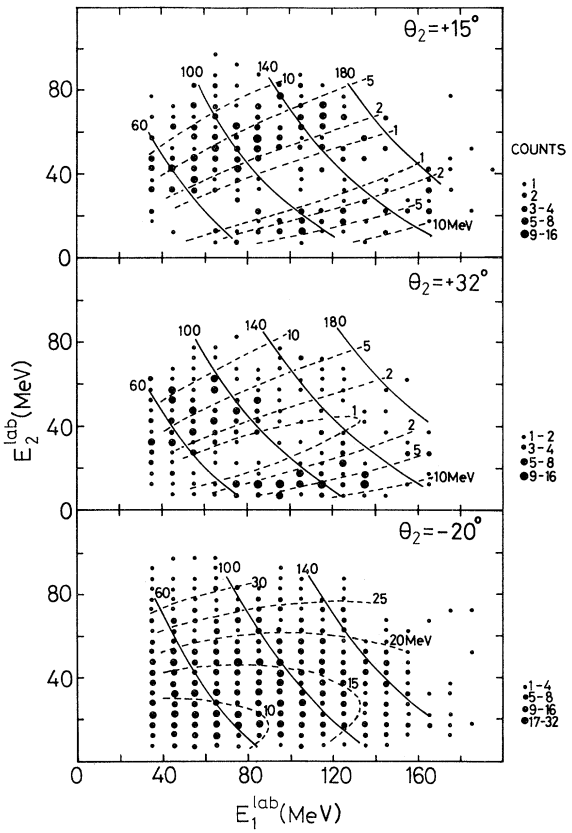

FIG. 3. The energy correlations between alpha particle and ^{12}C depicted in the plane of ^{12}C laboratory energy (E_1) vs alpha laboratory energy (E_2) for $\theta_1 = +22°$ and $\theta_2 = +15°$, $+32°$, and $-20°$. Count in each channel is indicated by the size of the dot. The dashed and solid lines represent the loci of the relative kinetic energy E_{1-2} between the alpha particle and ^{12}C and of the relative kinetic energy E_{12-3} between the center of mass of the composite system (α+ ^{12}C= ^{16}O) and its recoil nucleus, respectively.

distributed is peaked in two separate regions both corresponding to the same values of E_{1-2} (2—10 MeV) and E_{12-3} (60—140 MeV). This observation is consistent with the assumption of a sequential breakup mechanism, i.e., the assumption that the excited ^{16}O with the kinetic energy of 60—140 MeV and the excitation energy of 2—10 MeV in excess of the alpha threshold is produced strongly in the damped reaction, and subsequently breaks into the alpha particle and ^{12}C. Under this assumption two maxima should appear for a common intermediate state corresponding to the forward and backward emissions of the alpha particle with respect to the rest frame of the composite nucleus (^{16}O).

D. Projected energy spectra of the coincident alpha particles and ejectiles

A projected energy spectrum of the coincident particle i, $d^3\sigma/d\Omega_i d\Omega_j dE_i$, may be obtained for each set of (θ_i,θ_j) by integrating the coincidence cross section over E_j. Typical projected spectra of alpha particles in coincidence with various ejectiles are shown in Fig. 4. The shapes of the spectra depend very strongly on the detection angle θ_2 of the alpha particles. For the alpha particles detected in region II [Fig. 4(a)], the energy spectra show smooth distributions. They are approximately proportional to the singles spectra taken at the same angles, as shown by solid lines. This proportionality is generally observed for the data of region II over the different final channels as shown in Fig. 4(a). For the alpha particles detected in region I, energy spectra do not show such proportionality but show somewhat distorted shapes [see Fig. 4(b)] corresponding to the two hump structure observed for the energy correlation (Fig. 3).

Examples of projected energy spectra of the ejectiles may be seen in Fig. 5, which shows the results of ^{12}C obtained for various θ_2's. Qualitative conclusions drawn from these spectra are similar to those extracted from the projected alpha particle spectra. The energy spectra corresponding to region I show a two humped structure reflecting the nature of the energy correlation (Fig. 3). On the other hand, a smooth distribution of the ejectile energy spectrum is observed for the alpha particles detected in region II. The singles spectrum of ^{12}C detected at the same angle $\theta_1=+22°$ is shown for comparison. Note that the shapes of the projected spectra of ^{12}C are generally different from that of the singles spectrum, though the difference is less significant for the region II spectrum.

According to Eq. (1) the shape of the projected spectrum of the ejectile should always be identical to that of the singles spectrum independent of θ_2 when θ_1 is fixed. This is obviously not the case for the present reaction particularly for data of region I which shows the double humped structure. A similar comparison with singles spectra can be made for the alpha particles. For the data of region I, the projected spectra (Fig. 4) hardly resemble the corresponding singles spectra. On the other hand, the spectral shapes are rather similar between singles and coincidence spectra for the data of region II. This last feature is in accord with the expression in Eq. (1).

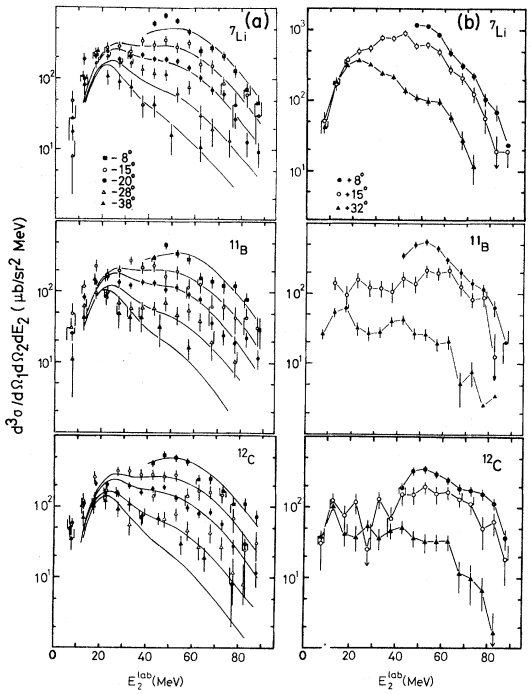

FIG. 4. The projected energy spectra of the alpha particles in coincidence with ^{7}Li, ^{11}B, and ^{12}C for the various angles θ_2. The solid lines in Fig. 4(a) represent the spectral shapes of the singles alpha particles for $\theta=8°$, 15°, 20°, 28°, and 38°, respectively. The solid lines in Fig. 4(b) only connect the data points.

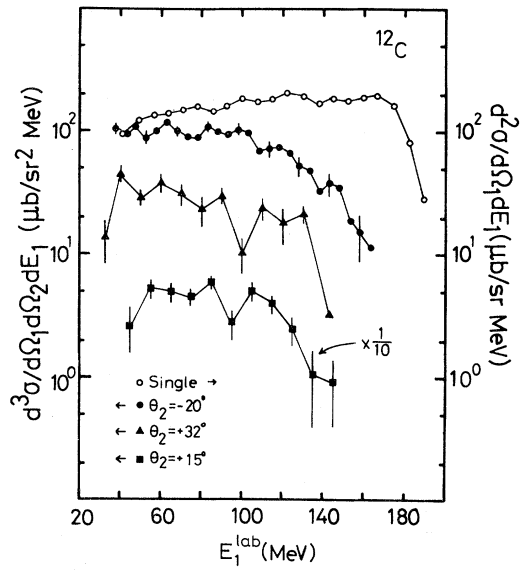

FIG. 5. The projected energy spectra for the ^{12}C ejectile detected at $\theta_1=+22°$ in coincidence with the alpha particles at $\theta_2=-20°$, $+32°$, and $+15°$. The singles spectrum of ^{12}C detected at the same angle $\theta_1=+22°$ is shown for comparison. The solid lines only connect the data points.

E. Alpha multiplicity

The relation between the singles and coincidence spectra as discussed in the previous subsection may be better depicted by the quantity R, which is defined as the ratio of the differential coincidence cross section $d^3\sigma/d\Omega_1 d\Omega_2 dE_1$ to the singles cross section $(d^2\sigma/d\Omega_1 dE_1)_{\text{singles}}$ for the same ejectile detected at the same angle $\theta_1 = +22°$ as for the coincidence measurement. If the relation of Eq. (1) is applicable, the ratio R should be constant with respect to E_1 and for different ejectiles. The differential alpha multiplicity $M_\alpha(E_1,\theta_1)$ may be obtained by integrating R over the solid angle Ω_2 of the alpha particle. This quantity represents the number of the alpha particle emitted per one event of an ejectile production with specific energy E_1 and angle Ω_1.

The ratios R for various ejectiles are plotted together in Figs. 6(a) and 6(b) as a function of E_1.

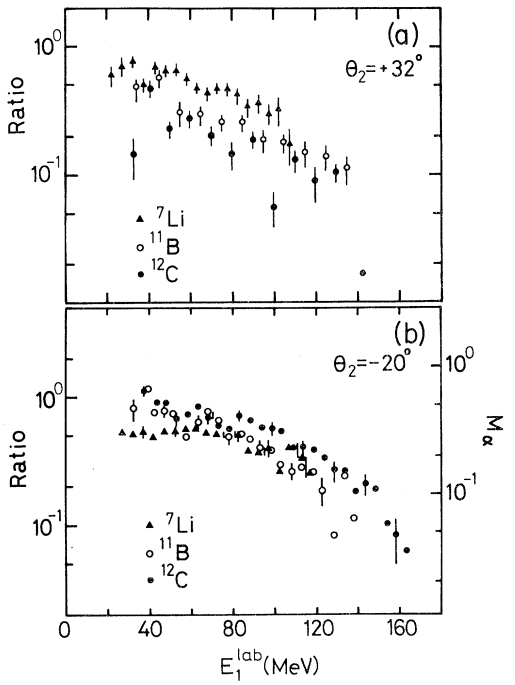

FIG. 6. The ratios of the differential coincidence cross section $d^3\sigma/d\Omega_1 d\Omega_2 dE_1$ integrated over the alpha particle energy E_2 to the singles differential cross section $(d^2\sigma/d\Omega_1 dE_1)_{\text{singles}}$ of the ejectiles detected at the same angle $\theta_1 = +22°$ as for the coincidence measurement, plotted as a function of the ejectile laboratory energy E_1. In Fig. 6(b) the estimated alpha multiplicity M_α, which is defined as the number of the alpha particles emitted per one event of an ejectile production with the specific energy E_1 and angle Ω_1, for region II is shown on the right hand side.

The results are again very different for region I [$\theta_2 = +32°$, Fig. 6(a)] and region II [$\theta_2 = -20°$, Fig. 6(b)]. For region I, the ratios R fluctuate strongly from ejectile to ejectile as well as with varied E_1. They also show a gross trend of decreasing rather sharply with increasing E_1. These features clearly conflict with the expectation of the fragmentation-like mechanism.

On the other hand the ratios R for region II show fairly simple behavior; they exhibit a nearly constant value (within $\pm 20\%$) in a wide region of E_1 and their dependence on type of ejectile is small. Only for the highest energies of E_1 they drop significantly. The fairly universal constancy of R implies that the coincidence cross section $d^3\sigma/d\Omega_1 d\Omega_2 dE_1$ is roughly proportional to the singles cross section of the corresponding ejectile and that the multiplication factor of alpha particles is similar for different ejectiles. As a matter of fact these features are the main implications of Eq. (1).

The multiplicity M_α is obtained by integrating R over Ω_2. M_α is shown on the right hand side of Fig. 6(b). Here we assumed that the out of plane correlation has the same distribution at different θ_2 as at $\theta_2 = -15°$, where the out of plane correlation was detected. The integration over θ_2 was limited to the region of $\theta_2 < 0°$, i.e., region II, since the events of region I may be more relevant to a different type of emission mechanism. Thus this multiplicity should be distinguished from the total multiplicity. It is seen in Fig. 6 that the multiplicities M_α are in the range of 0.3—0.6 in a wide low-energy region of E_1.

For region I we do not discuss M_α as defined in this way, because the sequential breakup may be dominant. In such a case, the alpha multiplicity defined with respect to the parent nucleus may have more significance than that to the detected ejectile as defined here. This will be discussed in Sec. IV C.

IV. THREE BODY KINEMATIC ANALYSIS

In the previous section, we have seen strong indications for the sequential ejectile breakup process particularly for data of region I. This process may be described as a two-step process consisting of the formation of an excited parent ejectile and its subsequent breakup into the observed alpha particle and ejectile. Such a process, which proceeds via an intermediate state, may be better described by

transforming the coordinate system from the laboratory frame into the rest frame of the parent fragment.[50] In the following, we first discuss the general properties characteristic of the transformation and then present the results of such three body kinematic analysis on the present data.

A. General remarks

We consider a reaction with three particles in the final channel. For the rest frame of the particles i and j, the coincidence cross section can be expressed as a function of E_{i-j}, E_{ij-k}, Ω_{i-j}, and Ω_{ij-k}. Here E_{i-j} is the relative kinetic energy of the particles i and j, E_{ij-k} is the relative kinetic energy of the center of the mass of the composite system $(i+j)$ and its recoil nucleus k, and Ω_{i-j} and Ω_{ij-k} are the corresponding solid angles. E_{i-j} corresponds to the excitation energy of the composite system $(i+j)$ that is in excess of the breakup threshold energy, whereas E_{ij-k} is related to the kinetic energy $E_{(i+j)}$ of the parent fragment $(i+j)$ in the center of mass of the three body system by

$$E_{(i+j)}=\frac{m_k}{m_i+m_j+m_k}E_{ij-k}\ , \tag{2}$$

where m_x represents the mass of the particle x.

The three body Q value Q_3 is given as $Q_3=E_p-(E_{i-j}+E_{ij-k})$, where E_p is the center of mass energy of the projectile.

The coincidence cross section in the rest frame of $(i+j)$ and in the laboratory frame is related by

$$d^4\sigma/d\Omega_{ij-k}d\Omega_{i-j}dE_{ij-k}dE_{i-j} = J\cdot d^4\sigma/d\Omega_i d\Omega_j dE_i dE_j\ , \tag{3}$$

where the Jacobian J is obtained by comparing the phase volumes between the two coordinate systems. The energy and angular variables for the rest frame of $(i+j)$ are related to the corresponding variables for the laboratory frame. Typical properties of these relations are graphically illustrated in Fig. 7, where contour lines of E_{12-3}, E_{1-2}, θ_{12-3}, and θ_{1-2} are drawn in the plane of E_1 and E_2 for the case where $\theta_1=+22°$ and $\theta_2=+32°$. The directions of θ_{12-3} and θ_{1-2} are also illustrated in Fig. 7.

The following remarks are made about the behavior of these contour lines:

(i) E_{1-2} has a low energy threshold $E^{\rm th}_{1-2}$, which is determined by E_{12-3} and the opening angle between θ_1 and θ_2. Therefore, the events with smaller E_{1-2}, if any, will be observed only when a sufficiently small opening angle $|\theta_1-\theta_2|$ is chosen.

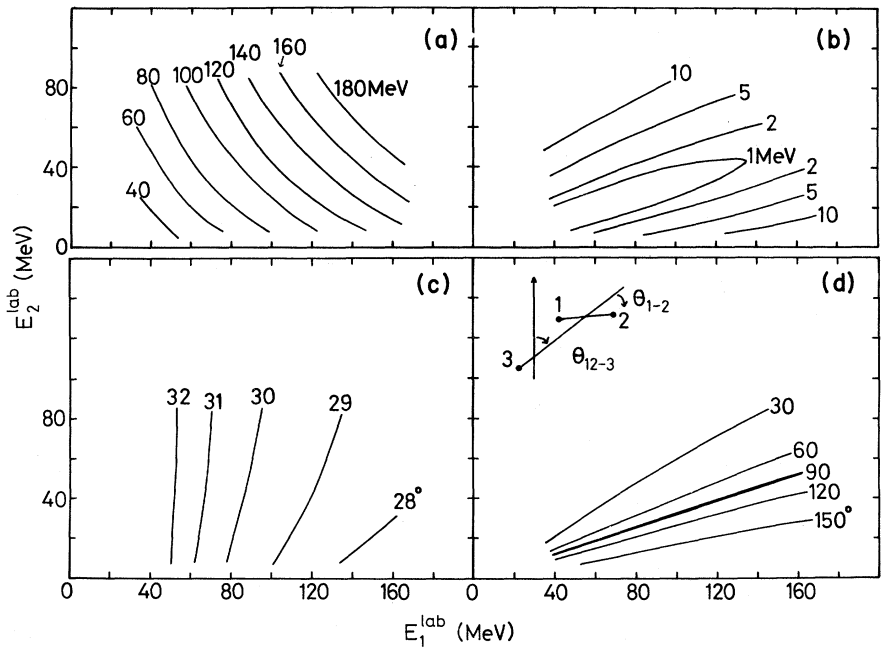

FIG. 7. The calculated loci of constant E_{12-3} (a), E_{1-2} (b), θ_{12-3} (c), and θ_{1-2} (d) based on the three body kinematics (Ref. 50) in the energy plane of ^{12}C vs alpha for $\theta_1=+22°$ and $\theta_2=+32°$. Here E_{1-2} and E_{12-3} are same as in Fig. 3, and θ_{1-2} and θ_{12-3} are corresponding angles, whose directions are also illustrated in the figure.

The simple average of E_{1-2} over the events taken at a given set of angles is generally affected by this threshold. In some of the earlier papers the average E_{1-2} value, which was strongly dependent on θ_2, i.e., on $|\theta_2-\theta_1|$, was wrongly used as evidence to rule out the sequential ejectile breakup mechanism.

(ii) A given set of (E_{1-2},E_{12-3}) generally appears at two points in the (E_1,E_2) plane unless the corresponding value of θ_{1-2} is 90°. These two points are located on opposite sides of the $\theta_{1-2}=90°$ line (thick solid line). Thus, if the cross section is primarily dependent on E_{1-2} and E_{12-3} and less on θ_{1-2} and θ_{12-3}, the contour plot of the cross section in the (E_1, E_2) plane should show a twofold pattern which is approximately symmetric with respect to the line with $\theta_{1-2}=90°$. Such a feature was indeed observed in the present data as shown in Fig. 3 ($\theta_2=+15°$ and $+32°$). By projecting the cross section over the (E_1, E_2) plane on either the E_1 or E_2 axis, one obtains the projected energy spectrum of the particle 1 or 2. Because of the twofold nature of the (E_1,E_2) plane, even the single peaked cross section in the plane of (E_{1-2},E_{12-3}) can result in a double humped structure of the projected spectrum on the E_1 or E_2 axis. The projected spectra of the alpha particles and ejectiles observed for the angular region I indeed show two peaks as described in Sec. III D [Figs. 4(b) and 5].

(iii) The value of θ_{1-2} varies significantly over the (E_1,E_2) plane. θ_{1-2} is larger than 90° in the (backward) domain between the E_1 axis and the line of $\theta_{1-2}=90°$, whereas it is smaller in the opposite (forward) domain. Two points of given values of (E_1,E_2) usually appear in the (E_1,E_2) plane, one in the forward domain and one in the backward domain. The angle θ_{12-3}, which represents the emission angle of the parent fragment, varies slightly towards more forward angles as E_1 (E_2) increases (decreases). In the sequential breakup process, the coincidence cross section in the (E_1,E_2) plane should be affected through θ_{12-3} by the angular dependence of the production yield of the parent nucleus. It is likely that the angular distribution of the primary excited fragment is similar to that of the same isotope detected in the singles measurement, which usually shows forward peaked behavior. Thus the cross sections $d^4\sigma/d\Omega_{12-3}d\Omega_{1-2}dE_{12-3}dE_{1-2}$ at the two points of the same (E_1,E_2) may differ from each other, the one for the forward domain being larger than the one for the backward domain.

B. E_{1-2} spectra

The E_{1-2} spectrum $d^3\sigma/d\Omega_{12-3}d\Omega_{1-2}dE_{1-2}$ was obtained for data of a given (θ_1, θ_2) by integrating the differential cross section $d^4\sigma/d\Omega_{12-3}d\Omega_{1-2}dE_{12-3}dE_{1-2}$ with respect to E_{12-3}. There the dependence of the cross section on θ_{1-2} was assumed to be constant. For a given set of (θ_1,θ_2) the angle θ_{12-3} may be regarded as a constant. Examples of E_{1-2} spectra are shown in Fig. 8. It is important to remember that the E_{1-2} spectrum is always affected by E^{th}_{1-2}, which causes the suppression of the observed coincidence cross section in the lowest region of E_{1-2}; E^{th}_{1-2} varies with the coincident ejectile and θ_2. Here we again note a distinct difference in the spectral shapes between the results for regions I and II.

The spectra of region I ($\theta_2=+15°$ and $+32°$) generally show fine structures of sharp spikes of peaks and dips. Many of the peaks appear at the

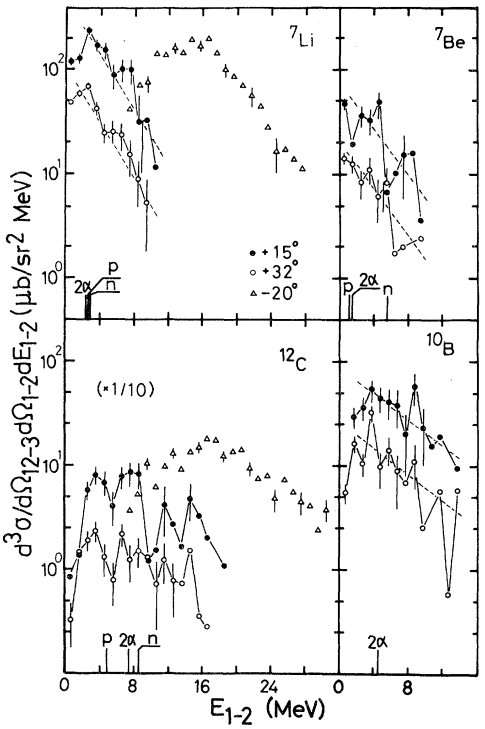

FIG. 8. The E_{1-2} spectra obtained by integrating the coincidence cross section $d^4\sigma/d\Omega_{12-3}d\Omega_{1-2}dE_{12-3}dE_{1-2}$ with respect to E_{12-3} for the various settings (θ_1,θ_2). The lines with "2α," "*n*," and "*p*" represent the threshold energies of the two-alpha particles, neutrons, and proton emission, respectively. The dashed lines are drawn using the form of $\exp(-E_{1-2}/T_{\text{eff}})$, where the values of T_{eff} are 2.8, 3.8, and 7 MeV for ^{7}Li, ^{7}Be, and ^{10}B, respectively.

same excitation energies, i.e., the same E_{1-2} when the angle set is varied for a given final channel. These peaks may correspond to excitations of discrete alpha decaying states of the parent nuclei. An attempt to identify these states with better energy resolution was discussed in a recent paper.[15] Because of the relatively poor energy resolution of the present data, we discuss only the gross features of the spectra. We observe that the spectra, after smoothing the fine structure, show fairly monotonous behavior of falling off towards larger E_{1-2} as depicted in Fig. 8 by the dashed lines which are proportional to $\exp(-E_{1-2}/T_{\text{eff}})$. It is important to note that these smoothed shapes are similar for spectra of the same final channel for different θ_2; T_{eff} is nearly independent of θ_2. This approximate independence of the spectral shape on θ_2 is a strong indication of the sequential breakup mechanism. The absolute magnitude of the cross section may depend on θ_2, since θ_{12-3} varies with θ_2 and the production yield of the parent nucleus may vary with θ_{12-3}. Based on these observations we try to formulate in Sec. V A a factorized expression of the coincidence cross section for the sequential breakup process.

The T_{eff} value depends significantly on the final channel, and increases with heavier ejectiles (2.8 MeV for ^{7}Li and 7 MeV for ^{10}B). This trend might be related to the variation in the threshold energies of the parent nuclei for emission of two alpha particles, neutrons, and protons. If the excitation energy of the primary fragment exceeds these energies, which are usually larger than the threshold energy of single alpha-particle emission, either a four-particle final state or a competing nucleon emission can become dominant. These threshold energies are indicated in Fig. 8.

At the lowest energies of E_{1-2} we observe a falling off of the cross section. This is mainly due to the effect of E^{th}_{1-2}, but may partly result from the Coulomb barrier between the alpha particle and the breakup partner.

In Fig. 9 we compare two E_{1-2} spectra of the $\alpha+{}^7$Li channel obtained for lower and higher E_{12-3}. The gross similarity observed in the high energy region of E_{1-2} may imply that the excitation pattern of the parent nucleus is not strongly dependent on the inelasticity of the primary reaction.

The E_{1-2} spectra (Fig. 8) for region II show some features which do not collaborate with those for region I. First, the cross section is absent in a wide low-energy region of the spectra. This is,

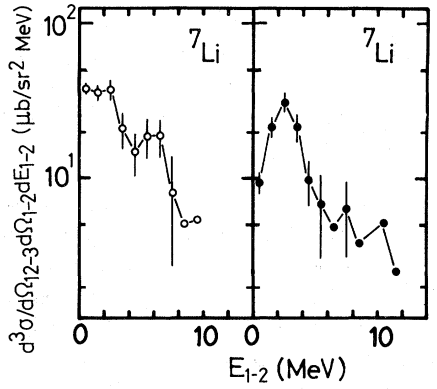

FIG. 9. The E_{1-2} spectra of the $\alpha+{}^7$Li channel obtained for the lower (25 MeV $\leq E_{12-3} < 75$ MeV, open circles) and higher ($E_{12-3} \geq 75$ MeV, closed circles) energy region of E_{12-3} for $\theta_1 = +22°$ and $\theta_2 = +32°$.

however, simply due to the geometrical effect associated with E^{th}_{1-2}. Besides that, one aspect remains clear: The cross section at higher E_{1-2} is extremely enhanced for region II. At $E_{1-2}=16$ MeV, for instance, the cross section of the $\alpha+{}^7$Li channel at $\theta_2 = -20°$ (region II) is a factor of 50 larger than that at $\theta_2 = +15°$ (region I).

This large difference in the cross section is hard to explain if we assume the same sequential breakup mechanism is important in region II as well as region I. Under such an assumption, the cross section difference should be primarily associated with the difference in the yield of the parent nucleus between emission angles θ_{12-3} corresponding to the angular sets (θ_1, θ_2) of the observed particles. The angle θ_{12-3} is typically 8° for $(\theta_1, \theta_2) = (+22°, -20°)$ and 24° for $(+22°, +15°)$. It is likely that the angular dependence of the parent nucleus yield is similar to that for the same isotope observed in the inclusive singles measurement. The singles angular distribution obtained for ^{11}B was forward peaked, showing an enhancement of a factor of 8 at 8° as compared to 24°. This enhancement is, however, hardly sufficient to account for the enhancement of the factor of 50 observed for the coincidence yield for region II. Thus it is reasonable to assume there is an additional mechanism attributing to the events in region II.

C. The E_{12-3} spectra

The E_{12-3} spectrum $d^3\sigma/d\Omega_{12-3}d\Omega_{1-2}dE_{12-3}$ was obtained by integrating the coincidence cross section $d^4\sigma/d\Omega_{12-3}d\Omega_{1-2}dE_{12-3}dE_{1-2}$ with

respect to E_{1-2} for specific (θ_1,θ_2) settings. Typical examples of the E_{12-3} spectra are shown in Fig. 10 for the case of $\alpha+{}^7$Li detected for $\theta_1=+22°$ and $\theta_2=+11°$, $+15°$, and $+32°$. The mean θ_{12-3} angles are, respectively, 21°, 24°, and 31°.

For the ejectile breakup mechanism, the E_{12-3} spectrum represents the kinetic energy spectrum of the parent fragment which is excited and eventually breaks up. Then it may be expected that the E_{12-3} spectrum resembles the singles energy spectrum of the corresponding fragment $(1+2)$ since the difference between the two spectra simply arises from whether or not the fragment is excited above the threshold of alpha particle breakup. To examine this aspect, we plot in Fig. 11 the ratios R of the coincidence cross sections $\int(d^3\sigma/d\Omega_{12-3}d\Omega_{1-2}dE_{12-3})d\Omega_{1-2} = 4\pi\cdot d^2\sigma/d\Omega_{12-3}dE_{12-3}$ to the singles cross sections $(d^2\sigma/d\Omega_{12-3}dE_{12-3})_{\text{singles}}$ taken at the same angle as θ_{12-3} for the cases of $\alpha+{}^7$Li (^{11}B), $\alpha+{}^{11}$B (^{15}N), and $\alpha+{}^{12}$C (^{16}O). This coincidence cross section was taken to represent the total probability of the alpha decay of the parent nucleus emitted at the given θ_{12-3} with given E_{12-3}. The factor 4π was taken to represent the angular integration over Ω_{1-2}. However, this factor might be too large because of the expected enhancement of the in plane correlation as compared to the out of plane correlation.

In this plot, the constancy of the ratio will imply that the coincidence cross section is proportional to

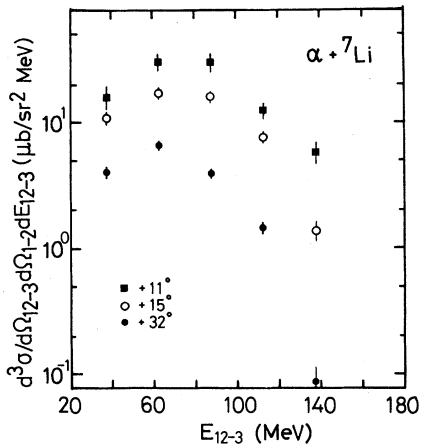

FIG. 10. The E_{12-3} spectra of the $\alpha+{}^7$Li channel obtained by integrating the coincidence cross section $d^4\sigma/d\Omega_{12-3}d\Omega_{1-2}dE_{12-3}dE_{1-2}$ with respect to E_{1-2} for $\theta_1=+22°$ and $\theta_2=+11°$, $+15°$, and $+32°$. The corresponding angles θ_{12-3} are 21°, 24°, and 31°, respectively.

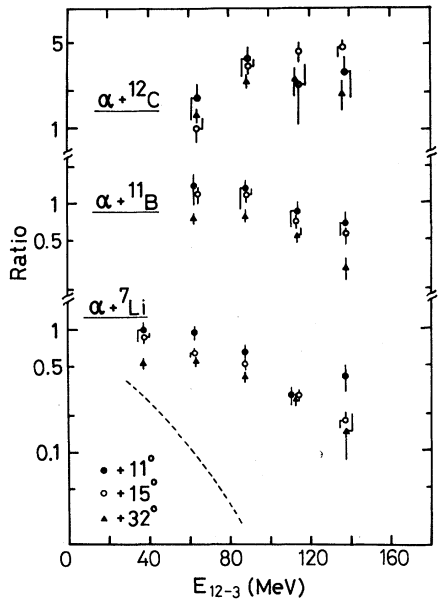

FIG. 11. The ratios of the coincidence cross section $\int(d^3\sigma/d\Omega_{12-3}d\Omega_{1-2}dE_{12-3})d\Omega_{1-2}$ to the singles cross section $(d^2\sigma/d\Omega_{12-3}dE_{12-3})_{\text{singles}}$ taken at the same angles as θ_{12-3} for $\alpha+{}^7$Li, $\alpha+{}^{11}$B, and $\alpha+{}^{12}$C channels as a function of E_{12-3}. The dashed line represents the ratio for the $\alpha+{}^7$Li channel at $\theta_2=-20°$ for comparison.

the singles cross section. This ratio is to be distinguished from that discussed in Sec. III E; here, the cross section is compared to the parent fragment, i.e., the particle $(1+2)$ rather than to the observed ejectile 1 in the case in Sec. III E. In a fairly wide energy region of E_{12-3}, the ratios are indeed nearly constant (within $\pm 25\%$) for the data of region I. For comparison, this ratio for $\theta_2=-20°$ (region II) is also shown for the $\alpha+{}^7$Li channel. In contrast the ratio for this angle varies significantly as a function of E_{12-3}.

From the ratio discussed above, we can determine the fraction f of the parent nucleus which decays by the alpha particle emission using the relation $f=R/(1-R)$. Note this fractional ratio f is much larger for the $\alpha+{}^{12}$C channel than for any other channels. This enhancement may indicate particular concentration in ^{16}O of alpha cluster states near the particle threshold that favorably decay into $\alpha+{}^{12}$C. This feature may be related to the observation[10,13,16] that in the ^{16}O induced reactions, the $\alpha+{}^{12}$C final channel usually has an enhanced coincidence yield and the primary process can be ascribed to the sequential breakup mechanism.

The dependence of the coincidence cross section on the three body reaction Q value Q_3 is inferred

from the spectra of $d^3\sigma/d\Omega_{12-3}d\Omega_{1-2}dE_{12-3}$. Since Q_3 is related to E_{12-3} through the equation $Q_3=E_p-(E_{1-2}+E_{12-3})$ as described in Sec. IV A, and since E_{1-2} is usually negligibly small as compared to E_{12-3}, the cross sections $d\sigma/d(-Q_3)$ and $d\sigma/dE_{12-3}$ are almost identical. As inferred from Fig. 10 as well as Fig. 11, the cross sections $d\sigma/d(-Q_3)$ are generally peaked at the larger $(-Q_3)$ values, indicating that the coincidence events are associated with highly inelastic processes. This feature is even the case for the $\alpha+{}^{10}$B channel which can be affected by the elastic projectile breakup. This particular breakup process, which leaves the target as a spectator, was found to have a significant cross section in the case of ^{20}Ne and ^{16}O induced reactions.[13,51] In contrast, it appears that the projectile breakup process is considerably weaker in the present reaction system of ^{93}Nb+ ^{14}N, at least for the observed angle (θ_1,θ_2) settings.

V. PROPERTIES OF TWO COMPETING MECHANISMS OF ALPHA EMISSION

In the previous sections, we have seen several features which consistently indicate that two significantly different mechanisms participate in the emission of the coincident alpha particles, one being dominant in the angular region I and the other in region II. In this section, we first summarize the properties of these two mechanisms separately. We then discuss the relative strength of these components.

A. The mechanism relevant to region I

The characteristic properties of the coincidence events detected for the geometry, where θ_2 is close to θ_1 (region I) are summarized as follows:

(i) Energy-energy correlations of the alpha particles and ejectiles show two humped patterns (Fig. 3). The projected energy spectra of both alpha particles and ejectiles show the double humped spectral shapes, which are significantly different from the singles energy spectra [Figs. 4(b) and 5].

(ii) The E_{1-2} spectra show peaks of fine structure which may be ascribed to the alpha decay of isolated excited states of the $(1+2)$ nucleus (Fig. 8).

(iii) The global shape of the E_{1-2} spectra, which is roughly expressed in the form of $\exp(-E_{1-2}/T_{\text{eff}})$, is almost independent of the detection angles of the coincident alpha particles (Fig. 8). Its dependence on E_{12-3} seems also to be weak (Fig. 9).

(iv) The ratio of the coincidence cross section $d^3\sigma/d\Omega_{12-3}d\Omega_{1-2}dE_{12-3}$ to the singles cross section of the parent fragment $(1+2)$ is roughly constant for a wide region of E_{12-3} and for different θ_2's (Fig. 11), whereas the ratio to the observed ejectiles 1 fluctuates significantly [Fig. 6(a)]. As discussed in the previous sections, all these features are consistent with the assumption that the reaction proceeds via a sequential ejectile breakup mechanism.

The features described in (iii) and (iv) lead us to formulate a semiquantitative expression for the coincidence cross section for this reaction mechanism. The feature of (iii) may imply that the cross section is simply a function of E_{1-2} and is independent of θ_{12-3} and E_{12-3}, whereas the feature of (iv) may imply that the dependence of the cross section on θ_{12-3} and E_{12-3} is given by the singles differential cross section $(d^2\sigma/d\Omega_{12-3}dE_{12-3})_{\text{singles}}$ of the nucleus corresponding to the composite system of the alpha particle plus ejectile. Thus, we obtain an approximate relation

$$d^4\sigma/d\Omega_{12-3}d\Omega_{1-2}dE_{12-3}dE_{1-2}=N\cdot f(E_{1-2})(d^2\sigma/d\Omega_{12-3}dE_{12-3})_{\text{singles}}\ , \tag{4}$$

where N is supposed to be a constant. In this argument, it is implicitly assumed that the angular distribution of the breakup process is isotropic in the reaction plane in the rest frame of the $(1+2)$ system, i.e., $d\sigma/d\Omega_{1-2}$ is constant. It is indeed likely that the angular distribution is isotropic at least in the reaction plane, because the spin alignment (or polarization) of the ejectiles is expected to be perpendicular to the reaction plane in view of the classical nature of the heavy-ion damped reactions.

B. The mechanism for region II

The coincidence events which were recorded with the alpha detector on the opposite side of the beam axis from the ejectile detector (region II) re-

vealed properties very different from those for the region I. These events do not show any of the features characteristic of the sequential breakup process, which are summarized in the preceding subsection. Instead, they show the following features: (i) The projected energy spectra of coincident alpha particles, $d^3\sigma/d\Omega_1 d\Omega_2 dE_2$, have shapes almost identical to those of the singles spectra $(d^2\sigma/d\Omega_2 dE_2)_{\text{singles}}$ taken at the same angles. (ii) This feature is even the case for projected spectra obtained in coincidence with particles with different energies E_1. In Fig. 12, the energy spectra of the alpha particles at $\theta_2 = -20°$ in coincidence with ^{12}C particles with energies above and below $E_1^{\text{lab}} = 77.5$ MeV are compared. The spectral shapes are similar to each other and to the singles spectrum. (iii) The same is true to a lesser extent for the projected spectra of ejectiles except for higher-energy regions.

These features are all consistent with the expression of Eq. (1). The values obtained from the present data for K in Eq. (1) are 0.31–0.48/b for various ejectiles. A similar value of $K = 0.5$/b was obtained for the ^{58}Ni + ^{14}N reaction in Ref. 8. Here it should be stressed again that the above expression is only valid for the data of region II and not over the entire angular region as in the case of Ref. 8. The contribution of this reaction mechanism to region I will be examined in the subsequent subsection.

In the present stage of understanding, it appears difficult to specify the detailed nature of the reaction process (fragmentationlike process) in region II. Based on the features characterized by Eq. (1), the authors of Ref. 8 inferred that the reaction may proceed in two steps in which the alpha particle is emitted at an early stage of the reaction in the projectile fragmentation process and the rest of the projectile subsequently undergoes damped reaction with the target. The feature of (ii) is in accord with this conjecture because the alpha-particle spectrum may be unaffected by the subsequent damped reaction, which controls the final energy of the emitted ejectile. This conjecture is also in harmony with the spirit of the recent theoretical attempts[52,53] to describe various breakup processes and massive transfer reactions in a unified framework. However, it is not obvious that such a two step reaction process will simply lead to the factorization formula in Eq. (1), which implies the "uncorrelated" emissions of the alpha particles and the ejectiles. It may be possible that the alpha particles and the ejectiles are emitted rather in a correlated manner via a recoil effect in the fragmentation process; the alpha particle may tend to be emitted on the opposite side of the beam from the ejectile as was observed in this experiment.

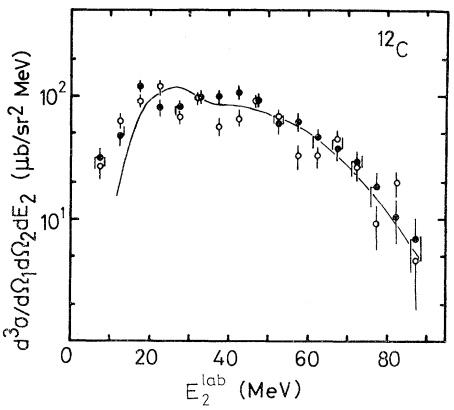

FIG. 12. The projected energy spectra of the alpha particles at $\theta_2 = -20°$ in coincidence with the lower ($E_1^{\text{lab}} < 77.5$ MeV, open circles) and higher ($E_1^{\text{lab}} \geq 77.5$ MeV, closed circles) energy ^{12}C particles. The solid line represents the spectral shape of the singles alpha particles for $\theta = 20°$.

C. The relative strength of two competing mechanisms

As summarized in the previous subsections, coincident alpha particles may be associated with two different mechanisms, i.e., the ejectile breakup mechanism and the fragmentationlike mechanism. These two components are, respectively, dominant in the angular regions I and II, but their fractions may well extend to the opposite regions. In this subsection we attempt to estimate the angular distribution of each of the two components, and examine their relative strength over the entire angular range.

Division of the total angular distribution into two components was recently discussed for the reaction ^{159}Tb + ^{14}N at 140 MeV in Ref. 15. These authors first assumed the angular distribution of the fragmentationlike process following the form of Eq. (1), which is symmetric with respect to the beam direction. The total angular distribution was then assumed to be the superposition of an ejectile breakup distribution and a symmetric distribution. According to these assumptions the peak of the total angular distribution should shift from the beam direction towards the side of the angular region where the ejectile breakup becomes important. This conclusion, however, did not always hold for the present data, as mentioned in Sec. III B. For

instance, in several final channels such as $\alpha + {}^{12}C$ and $\alpha + {}^{13}C$, the peak of the distribution appeared at a negative angle of θ_2 although the ejectile breakup component was found to be more intense at positive angles. This observation implies that the fragmentationlike component by itself peaks on the side with negative angles; this is different from the predictions of Eq. (1). Thus, the following we start by evaluating the ejectile breakup distribution, in contrast to the procedure used in Ref. 15.

In principle, the component of the ejectile breakup may be distinguished by inspecting the E_{1-2} spectrum obtained with sufficient energy resolution, where the relevant events manifest themselves as discrete lines on the continuous spectrum which in turn represents the other types of mechanisms. Such an analysis was indeed reported for the $^{159}Tb + 140$ MeV ^{14}N reaction,[15] where coincidences were observed between alpha particles at 30.5° and ejectiles at 20°. For this specific backward angle of θ_2, most events were ascribed to discrete lines and consequently to the ejectile breakup mechanism.

In the present measurement the angular resolution was relatively poor so that the energy resolution in the resultant E_{1-2} spectrum was insufficient to reliably perform the above type of analysis. Instead we make use of the relation in Eq. (4) discussed in Sec. V A to calculate the angular distribution of the ejectile breakup. In Sec. V A Eq. (4) was only applied to events of region I. However, the same relation may be applicable to events over the entire angular region as far as the ejectile breakup component is concerned.

In Fig. 13 the angular distribution of the ejectile breakup component calculated for the $\alpha + {}^{7}Li$ channel is indicated by a solid line. In the calculation the E_{1-2} spectrum obtained for $\theta_2 = +32°$ and the inclusive differential cross sections of ^{11}B obtained from a separate measurement[54] were, respectively, used for $f(E_{1-2})$ and $(d^2\sigma/d\Omega_{12-3}dE_{12-3})_{\text{singles}}$ in Eq. (4). The normalization was made at $\theta_2 = +32°$ assuming that the ejectile breakup mechanism is totally responsible for the coincidence cross section at this angle. The comparison with the experimental result as indicated by open circles shows that the calculated line only accounts for a part of the observed cross section particularly in region II. One may attribute a tiny fraction of the remaining part to the sequential decay of the equilibrated targetlike fragment as indicated by the dotted-dashed line. This line was obtained by extrapolation of the coincidence cross

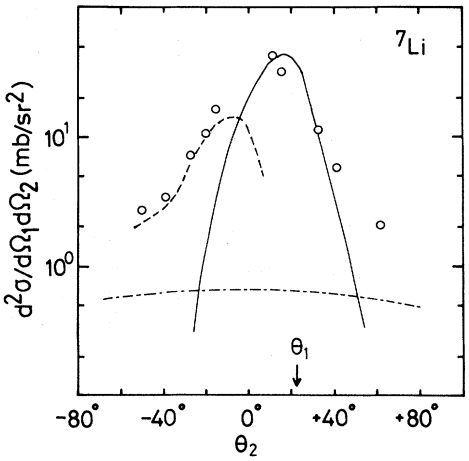

FIG. 13. The angular distribution of alpha particles in coincidence with ^{7}Li ejectiles (open circles) and the calculated angular distribution of the ejectile breakup component (solid line) obtained from Eq. (4) for the $\alpha + {}^{7}Li$ channel (see text). The dotted-dashed line represents the sequential decay from the equilibrated targetlike fragment. The remaining part of the experimental data as deduced by subtracting the above two components is indicated by the dashed line.

section at a far backward angle of $\theta_2 = -160°$ where the sequential decay from the targetlike fragment may only be available. By subtracting the contributions from the ejectile breakup and the decay of the targetlike fragment we are left with the contribution of the fragmentationlike mechanism, which has about the same strength as the ejectile breakup mechanism.

The quantitative accuracy of the calculation is somewhat dubious because of the simplifications involved in the formulation of Eq. (4). In particular the assumption that the function $f(E_{1-2})$ has no dependence on E_{12-3} may be an extreme simplification since population of the unbound excited states of the parent nucleus may tend to be reduced as E_{12-3} increases, i.e., as the inelasticity decreases. The $f(E_{1-2})$ spectrum used in the calculation was taken from the data at $\theta_2 = +32°$, where the coincidence events were mainly associated with the fully damped component of the ejectile. Thus, the calculated results can be an overestimation for the negative angular region of θ_2 (region II), where the corresponding angles of θ_{12-3} become more forward so that a larger contribution from the quasielastic component is expected. If this argument is correct, the angular distribution of the ejectile breakup component becomes narrower than the calculated distribution by being further suppressed

in region II. Accordingly, the strength of the other component becomes larger than indicated by the dashed line.

We have made similar analyses on several other channels. In spite of the uncertainties involved we make the following observations based on these analyses: (i) The angular distribution of the fragmentationlike component tends to be peaked at a negative angle of θ_2 instead of $\theta_2=0°$ as expected from Eq. (1). (ii) The relative strength between the two components varies within a factor of about 2 depending upon the final channel.

VI. SUMMARY AND DISCUSSION

In the previous sections it was shown that there are two types of important emission mechanisms contributing to the coincident alpha particles observed in the ^{93}Nb+ ^{14}N reaction at 208 MeV. The first mechanism was ascribed to the sequential breakup of the ejectiles which were produced in their unbound excited states in the primary binary reactions. The alpha particles due to this mechanism were most strongly populated in the angular region in the vicinity of the ejectile detector (region I). The second component of the alpha particles may be classified as the analog to the fragmentationlike process as denoted by the authors of Ref. 8. The alpha particles of this category were most significant at angles on the opposite side of the ejectile detector with respect to the beam direction (region II). At these angles the coincident alpha particles exhibited the differential cross sections which approximately followed the form of Eq. (1) as in the case of Ref. 8.

The relative contribution of the two mechanisms was examined and found to be roughly comparable, though it was slightly dependent on the final channel. The variation of the relative strength with final channel is not surprising in view of the following consideration: For a given final channel $\alpha+b$ the strength of the ejectile breakup component is governed by the production yield of the composite nucleus $(\alpha+b)$ in its excited states, while that for the other component is associated with the yield of the nucleus b. Since the yields of b and $(\alpha+b)^*$ are not generally correlated, the competition between the two types of alpha particles can easily fluctuate with the choice of b.

In the recent correlation studies on the reactions ^{197}Au+ ^{16}O at 310 MeV (Ref. 13) and ^{93}Nb+ ^{16}O at 204 MeV,[10] the coincident alpha particles were totally ascribed to the sequential ejectile breakup. On the other hand the coincident alpha particles in the ^{58}Ni+ ^{14}N reaction at 148 MeV (Ref. 8) were mainly associated with the fragmentationlike mechanism. In a more recent study of another ^{14}N induced reaction[15] on ^{159}Tb, the coexistence of the two components was reported in agreement with the present conclusion. Comparing these data we find that the competition between the two different mechanisms is strongly dependent on projectile and that the ejectile breakup process is particularly intense for the reactions with the ^{16}O projectile. For ^{16}O induced reactions the coincidence cross section is much larger for the $\alpha+$ ^{12}C channel than the other channels so that the data were usually analyzed only for that particular channel; the cross section for $\alpha+$ ^{12}C in the ^{16}O induced reactions is also extremely enhanced as compared to the various final channels in the ^{14}N induced reactions. The enhancement of the $\alpha+$ ^{12}C cross section for the ^{16}O projectile and its origin being ejectile breakup appears to comply with an observation made on the present data. As discussed in Sec. IV C, we found that the probability of ejectile breakup is significantly higher for the ^{16}O product than for any other product nucleus. This feature may be almost independent of the projectile used to produce the resultant nuclei. In the case of the ^{16}O induced reaction the production yield of ^{16}O in the primary binary reaction may be very large since it is associated with the inelastic channel. Thus one can expect a large yield of $\alpha+$ ^{12}C arising from the sequential breakup of ^{16}O.

In the ^{14}N induced reactions the contribution from the fragmentationlike process is also significant. The authors of Ref. 8 inferred that this process proceeds in two steps, i.e., through the projectile fragmentation followed by the "deep inelastic" reaction between the fragment and the target. Their inference was primarily based on the observation that the coincidence cross sections can be factorized with the singles cross sections of the alpha particle and ejectile; this indicates that the processes of producing the two coincident partners are isolated from each other, i.e., are uncorrelated. In the present study, we found that the behavior of the fragmentationlike component deviated slightly from the expectation of Eq. (1); the cross section is somewhat suppressed on the same side of the beam as the ejectile detector and peaking on the opposite side. This feature of correlation, however, may not necessarily conflict with the idea of the two step

process as suggested in Ref. 8; it is rather unlikely that the initial correlation in momentum between the fragments embedded in the projectile can be totally wiped out during the succeeding fragmentation and deep inelastic processes.

In the argument of the fragmentationlike mechanism in Ref. 8, no explanation was offered for the fragmentationlike mechanism. The theory[53] of the "breakup fusion" mechanism may have some relevance to such a mechanism. In this theory, which was recently proposed to account for the fast alpha particles observed in the singles measurement, the alpha particles were supposed to arise from a two-step process in which the projectile is first broken up into the alpha particle and its counterpart and then the former comes out as an ejectile while the latter fuses into the target. The natural extension of this theory may be to ascribe the fragmentationlike process to the projectile breakup followed by the "deep inelastic" reaction between the target and the counterpart of the alpha particle. If such a process is relevant to the present ^{14}N induced reaction studies, the cross section may be significantly enhanced in the $\alpha+{}^{10}$B channel as compared to, say, $\alpha+{}^{12}$C; the breakup fragment ^{10}B may undergo the inelastic reaction more favorably than the pickup reaction in the second step deep inelastic process as expected from the systematic trend of the cross section observed for the relatively light projectile ($A \lesssim 20$) induced deep inelastic reactions. The observed result, however, was rather contradictory with this expectation; there is no particular enhancement of the cross section in the $\alpha+{}^{10}$B channel. Thus it appears that the naive picture of the "breakup" induced mechanism is too simple.

The importance of the breakup induced mechanism may also be inferred on the basis of the strength of the component of the elastic projectile breakup. This component may be identified as the event with the three body Q value $Q_3 = Q_{ggg}$, where Q_{ggg} is the ground state Q value of the three body final channel. For the present data on $\alpha+{}^{10}$B, most coincidence events were associated with $(-Q_3)$ larger than 30 MeV, and the fraction of $Q_3 \sim Q_{ggg}$ was found to be at most 10%. This result indicates the projectile breakup process and also the various mechanisms associated with that process are not significant.

The coincident alpha particles so far discussed in terms of the fragmentationlike mechanism might be related to the emission from the "hot spot" created in the target nucleus via the primary reaction. Such an idea was postulated to account for the correlation data from the reaction of ^{58}Ni$+{}^{16}$O at 96 MeV. In order to examine this aspect we have calculated the energy and angular correlations from the hot spot model as discussed in Ref. 25. We find, as described below, that such a calculation indeed can give rise to a reasonable fit to the present data of region II. This observation is rather surprising in view of the difference in nature between the hot spot mechanism and the fragmentationlike mechanism: The alpha particle emission is supposed to arise from the target nucleus for the hot spot mechanism, but from the projectile for the fragmentationlike mechanism. Moreover, the emission for the former mechanism occurs in the latter stage of the presumed two step reaction, while that for the latter in the primary stage.

For our calculations the hot spot model in Ref. 25 was somewhat modified. The main modification was concerned with the assumption as to how the angular momentum is carried after the formation of the hot spot; we assumed that it is carried by the hot spot alone instead of the total target system as assumed in the original paper. Consequently, a smaller moment of inertia was used in the present calculation giving rise to a faster rotational speed for the center of mass of the hot spot. Because of this fast motion of the hot spot the backward emission of the alpha particle was highly suppressed as viewed from the laboratory system essentially yielding the single peaked angular distribution of the coincident alpha particle as observed experimentally. This result is in contrast to the double peaked angular distribution which was predicted by the original calculation in Ref. 25 and was sometimes referred to as the characteristic property of the hot spot mechanism. The projected energy spectra of the coincident alpha particles at various angles were also reproduced fairly well in the present calculation. Aside from these positive aspects, the calculation also involved some inconveniences. In particular, we had to assume the positive deflection angle of the primary "deep inelastic" scattering to achieve a reasonable fit to the data. Apparently this assumption conflicts with the usual prescription that the deep inelastic process favorably proceeds through the negative angle deflection.

Under the present maturity of the theories it is difficult to conclude either the fragmentationlike or the hot spot approach is more adequate to describe the nonsequential component of the alpha

particles. It is even probable that both types of mechanisms participate in the reaction. In order answer these questions, further elaboration of the theories is obviously important. At the same time it may be desirable to accumulate more systematic data on the correlation over a broader variety of the reaction systems and experimental conditions. Such studies would hopefully yield new types of information which may help to distinguish the underlying reaction mechanisms.

ACKNOWLEDGMENTS

We wish to thank the late Director S. Yamabe for his continuous encouragement throughout this work. We gratefully acknowledge Dr. M. Inoue and Dr. S. Nakayama and the cyclotron crew for their kind help. We also thank Dr. T. Nomura, Dr. K. Katori, and Dr. T. Shimoda for valuable discussions. This experiment was performed at Research Center for Nuclear Physics, Osaka University under Programs No. 4A-6 and 9A-8.

[1]D. C. Slater, J. R. Hall, J. R. Calarco, B. A. Watson, and J. A. Becker, Phys. Rev. Lett. 33, 784 (1974).

[2]R. Ost, N. E. Sanderson, S. Mordechai, J. B. A. England, B. R. Fulton, J. M. Nelson, and G. C. Morrison, Nucl. Phys. A265, 142 (1976).

[3]J. W. Harris, T. M. Cormier, D. F. Geesaman, L. L. Lee, Jr., R. L. McGrath, and J. P. Wurm, Phys. Rev. Lett. 38, 1460 (1977).

[4]H. Ho, R. Albrecht, W. Dünnweber, G. Graw, S. G. Steadman, J. P. Wurm, D. Disdier, V. Rauch, and F. Scheibling, Z. Phys. A 283, 235 (1977).

[5]T. Shimoda, M. Ishihara, H. Kamitsubo, T. Motobayashi, and T. Fukuda, in Proceedings of the IPCR Symposium on Macroscopic Features of Heavy-Ion Collisions and Pre-Equilibrium Process, Hakone, 1977, edited by H. Kamitsubo and M. Ishihara (unpublished), p. 93.

[6]C. K. Gelbke, M. Bini, C. Olmer, D. L. Hendrie, J. L. Laville, J. Mahoney, M. C. Mermaz, D. K. Scott, and H. H. Wieman, Phys. Lett. 71B, 83 (1977).

[7]R. K. Bhowmik, E. C. Pollacco, N. E. Sanderson, J. B. A. England, and G. C. Morrison, Phys. Lett. 80B, 41 (1978).

[8]R. K. Bhowmik, E. C. Pollacco, N. E. Sanderson, J. B. A. England, and G. C. Morrison, Phys. Rev. Lett. 43, 619 (1979).

[9]R. Billerey, C. Cerruti, A. Chevarier, N. Chevarier, B. Cheynis, and A. Demeyer, Z. Phys. A 292, 293 (1979).

[10]G. R. Young, R. L. Ferguson, A. Gavron, D. C. Hensley, Felix E. Obenshain, F. Plasil, A. H. Snell, M. P. Webb, C. F. Maguire, and G. A. Petitt, Phys. Rev. Lett. 45, 1389 (1980).

[11]H. Ho, P. Gonthier, M. N. Namboodiri, J. B. Natowitz, L. Adler, S. Simon, K. Hagel, R. Terry, and A. Khodai, Phys. Lett. 96B, 51 (1980).

[12]H. Gemmeke, P. Netter, Ax. Richter, L. Lassen, S. Lewandowski, W. Lücking, and R. Schreck, Phys. Lett. 97B, 213 (1980).

[13]M. Bini, C. K. Gelbke, D. K. Scott, T. J. M. Symons, P. Doll, D. L. Hendrie, J. L. Laville, J. Mahoney, M. C. Mermaz, C. Olmer, K. Van Bibber, and H. H. Wieman, Phys. Rev. C 22, 1945 (1980).

[14]A. Gavron, R. L. Ferquson, Felix E. Obenshain, F. Plasil, G. R. Young, G. A. Petitt, K. Geoffroy Young, D. G. Sarantites, and C. F. Maguire, Phys. Rev. Lett. 46, 8 (1981).

[15]J. van Driel, S. Gonggrijp, R. V. F. Janssens, R. H. Siemssen, K. Siwek-Wilczynska, and J. Wilczynski, Phys. Lett. 98B, 351 (1981).

[16]M. Sasagase, M. Sato, S. Hanashima, K. Furuno, Y. Nagashima, Y. Tagishi, S. M. Lee, and T. Mikumo (unpublished).

[17]R. K. Bhowmik, E. C. Pollaco, J. B. A. England, G. C. Morrison, and N. E. Sanderson, Nucl. Phys. A363, 516 (1981).

[18]J. M. Miller, G. L. Catchen, D. Logan, M. Rajagopalan, J. M. Alexander, M. Kaplan, and M. S. Zisman, Phys. Rev. Lett. 40, 100 (1978).

[19]A. Gamp, J. C. Jacmart, N. Poffé, H. Doubre, J. C. Roynette, and J. Wilczynski, Phys. Lett. 74B, 215 (1978).

[20]Y. Eyal, A. Gavron, I. Tserruya, Z. Fraenkel, Y. Eisen, S. Wald, R. Bass, G. R. Gould, G. Kreyling, R. Renfordt, K. Stelzer, R. Zitzmann, A. Gobbi, U. Lynen, H. Stelzer, I. Rode, and R. Bock, Phys. Rev. Lett. 41, 625 (1978).

[21]D. Hilscher, J. R. Birkelund, A. D. Hoover, W. U. Schröder, W. W. Wilcke, J. R. Huizenga, A. C. Mignerey, K. L. Wolf, H. F. Breuer, and V. E. Viola, Jr., Phys. Rev. C 20, 576 (1979).

[22]B. Tamain, R. Chechik, H. Fuchs, F. Hanappe, M. Morjean, C. Ngô, J. Peter, M. Dakowski, B. Lucas, C. Mazur, M. Ribrag, and C. Signarbieux, Nucl. Phys. A330, 253 (1979).

[23]R. Ost, A. J. Cole, M. R. Clover, B. R. Fulton, and B. Sikora, Nucl. Phys. A342, 185 (1980).

[24]D. H. E. Gross and J. Wilczynski, Phys. Lett. 67B, 1 (1977).

[25]P. -A. Gottschalk and M. Weström, Phys. Rev. Lett. 39, 1250 (1977); R. Weiner and M. Weström, *ibid.* 34, 1523 (1975); Nucl. Phys. A286, 282 (1977).

[26]P. -A. Gottschalk and M. Weström, Nucl. Phys. A314, 232 (1979).

[27]W. J. Swiatecki, Erice Lectures, Lawrence Berkeley Laboratory Report LBL-8950, 1979.

[28]M. C. Robel, Ph. D. thesis, Lawrence Berkeley Laboratory Report LBL-8181, 1979.

[29]J. P. Bondorf, J. N. De, A.O.T. Karvinen, G. Fái, and B. Jakobsson, Phys. Lett. 84B, 162 (1979).
[30]J. P. Bondorf, J. N. De, G. Fái, A.O.T. Karvinen, B. Jakobsson, and J. Randrup, Nucl. Phys. A333, 285 (1980).
[31]H.C. Britt and A.R. Quinton, Phys. Rev. 124, 877 (1961).
[32]T. Inamura, M. Ishihara, T. Fukuda, T. Shimoda, and H. Hiruta, Phys. Lett. 68B, 51 (1977).
[33]D.R. Zolnowski, H. Yamada, S.E. Cala, A.C. Kahler, and T.T. Sugihara, Phys. Rev. Lett. 41, 92 (1978).
[34]T. Nomura, H. Utsunomiya, T. Motobayashi, T. Inamura, and M. Yanokura, Phys. Rev. Lett. 40, 694 (1978).
[35]T. Nomura, J. Delaunay, C. Tosello, and N. Bendjaballah, Nucl. Phys. A305, 262 (1978).
[36]L. Westerberg, D.G. Sarantities, D.C. Hensley, R.A. Dayras, M. L. Halbert, and J.H. Barker, Phys. Rev. C 18, 796 (1978).
[37]D.G. Sarantities, L. Westerberg, M.L. Halbert, R.A. Dayras, D.C. Hensley, and J. H. Barker, Phys. Rev. C 18, 774 (1978).
[38]K. Siwek-Wilczynska, E. H. du Marchie van Voorthuysen, J. van Popta, R.H. Siemssen, and J. Wilczyński, Phys. Rev. Lett. 42, 1599 (1979).
[39]J. Wilczynski, R. Kamermans, J. van Popta, R.H. Siemssen, K. Siwek-Wilczynska, and S.Y. van der Werf, Phys. Lett. 88B, 65 (1979).
[40]H. Yamada, D.R. Zolnowski, S.E. Cala, A.C. Kahler, J. Pierce, and T.T. Sugihara, Phys. Rev. Lett. 43, 605 (1979).
[41]T. Inamura, T. Kojima, T. Nomura, T. Sugitate, and H. Utsunomiya, Phys. Lett. 84B, 71 (1979).
[42]T.C. Awes, C.K. Gelbke, B.B. Back, A.C. Mignerey, K.L. Wolf, P. Dyer, H. Breuer, and V.E. Viola, Jr., Phys. Lett. 87B, 43 (1979).
[43]H. Utsunomiya, T. Nomura, T. Inamura, T. Sugitate, and T. Motobayashi, Nucl Phys. A334, 127 (1980).
[44]T.J.M. Symons, P. Doll, M. Bini, D.L. Hendrie, J. Mahoney, G. Mantzouranis, D.K. Scott, K. van Bibber, Y.P. Viyogi, H.H. Wieman, and C.K. Gelbke, Phys. Lett. 94B, 131 (1980).
[45]T.C. Awes, C.K. Gelbke, G. Poggi, B.B. Back, B. Glagola, H. Breuer, V.E. Viola, Jr., and T.J.M. Symons, Phys. Rev. Lett. 45, 513 (1980).
[46]B.B. Back, K.L. Wolf, A.C. Mignerey, C.K. Gelbke, T.C. Awes, H. Breuer, V.E. Viola Jr.,and P. Dyer, Phys. Rev. C 22, 1927 (1980).
[47]W. W. Morison, S.K. Samaddar, D. Sperber, and M. Zielinska-Pfabe, Phys. Lett. 93B, 379 (1980).
[48]S.I.A. Garpman, D. Sperber, and M. Zielinska-pfabe, Phys. Lett. 90B, 53 (1980).
[49]L.C. Northcliffe and R.F. Schilling, Nucl. Data A7, 233 (1970).
[50]G.G. Ohlsen, Nucl. Instrum. Methods. 37, 240 (1965).
[51]T. Udagawa, T. Tamura, T. Shimoda, H. Furöhlich, M. Ishihara, and K. Nagatani, Phys. Rev. C 20, 1949 (1979).
[52]K.-I. Kubo and T. Kishimoto, Bull. Am. Phys. Soc. 23, 16 (1978); and T. Kishimoto and K.-I. Kubo, Texas A & M Cyclotron Institute Annual Report, 1978, p. 36.
[53]T. Udagawa and T. Tamura, Phys. Rev. Lett. 45, 1311 (1980).
[54]T. Fukuda, M. Tanaka, M. Ishihara, H. Ogata, I. Miura, and H. Kamitsubo, Phys. Lett. 99B, 317 (1981).